

---

# OMEGA Upgrade Status Report

The completion (and acceptance by the Department of Energy) of the final design of the upgrade to the OMEGA laser system marks the beginning of the system-integration phase of the project. System integration is the manufacturing and installation of the various subassemblies that constitute the laser system. It began during this reporting period with the delivery and installation of the major structures. By the end of December, nearly all of the support structures were installed in the laser and target bays.

In November, all of the main target bay structures were installed, including the F-ASP monoliths, both end mirror structures, and the target mirror structure (TMS). During that time, the target chamber had to be installed within the TMS. To be completed are the personnel platform for the TMS and the periscope mirror assembly.

In the laser bay, nearly all of the structures were installed, including all the splitters, the amplifier and spatial filter structures for stages A through E, and the structures for the frequency converters. Left to install are four structures: one for the stage-F amplifiers and three for the stage-F spatial filters.

This issue of the LLE review continues the series begun in the last issue—the system description as excerpted from the Executive Summary provided to DOE as part of the review documentation of the OMEGA Upgrade design. This issue contains descriptions of subsystems including power conditioning, controls, optomechanical systems (both laser and target areas), and major structures.

## Power Conditioning

The power-conditioning subsystem converts utility ac electrical power into the high-voltage, high-current electrical pulses used to fire the flash lamps that supply optical pump energy to the laser amplifiers. To create these pulses, large capacitors are charged to high voltage (7 kV) and then dis-

charged through a pulse-forming network (PFN) comprising that capacitor, an inductor, and a flash-lamp pair.

The number of flash lamps used in each amplifier is dependent upon the size of the amplifier. Each PFN is connected to one, two, or five flash lamps, depending on whether it feeds a 15-cm, 20-cm, or rod amplifier, respectively. An assembly consisting of the PFN's, a charger, and the control circuitry needed to power one laser amplifier is referred to as a power-conditioning unit (PCU). This is a complete unit requiring only command instructions from the power-conditioning control computer and ac input power. A charging power supply in each PCU allows adjustment of the energy output of each amplifier; this level of control is required for balancing the power of the laser system.

In addition to the main discharge circuitry, many PCU's will have preionization and lamp check (PILC) circuits. This circuitry provides a lower energy pulse (higher voltage, lower current) that is fired 250  $\mu$ s before each normal system shot (preionization). This pulse ionizes the gas in the lamp in preparation for the large current pulse that will follow. The preionization provides a near full-bore discharge that reduces the production UV line radiation that is detrimental to amplifier lifetime. In addition, the acoustic shock from the electrical discharge is reduced when a PILC is used. The PILC discharge is also used alone after a shot to check for lamp failures on that shot (lamp check). The PCU has the circuitry required to monitor each lamp during this PILC discharge and detect any that do not conduct current; faulty lamps will be replaced prior to the next shot.

To ensure safe operation, each PCU has an extensive array of hard-wired logical interlocks and self-checks. This is complemented by a local microprocessor used to monitor the interlocks and the status of various voltages and currents. This PCU control module (PCM) is based on the Neuron<sup>®</sup> Chip

from Echelon Corporation. The module contains LON (local operating network) interface circuits, a trigger input receiver, a logic power supply, and fiber-optic transceivers for communication. The PCM is housed in a steel enclosure with an eight-character alphanumeric display to indicate the status of the PCU.

Because of the high voltages present in the power-conditioning subsystem, safety was a major concern during design. The PCU's are computer controlled for normal operation, but for safety there are a number of "hard-wired" interlocks that do not rely on computers for activation. For instance, each of the enclosures is interlocked, and the capacitor is immediately discharged when the interlock is violated.

At the normal operating voltages the power-conditioning system will be capable of storing 42 MJ of electrical energy. The system is rated for even higher voltages, storing 46.2 MJ at full rated voltages. The extra capability will accommodate future needs as amplifiers (and other components) degrade and require more pump energy to obtain the nominal stage gains.

The Upgrade power-conditioning system consists of 120 disk amplifier PCU's and 97 rod amplifier PCU's. There are two types of disk amplifiers and, hence, two styles of disk PCU's. The difference is the number of individual flash-lamp circuits (PFN's) required. The 20-cm SSA (single-segment amplifier) PCU requires 16 PFN's, while the 15-cm SSA PCU requires only 12 PFN's. Other than the number of PFN's the units are identical. The PCU's will store a maximum of 368 kJ (20 cm) or 276 kJ (15 cm) at 14.8 kV.

There will be two styles of PCU's for the rod amplifiers. One type will power the stage-D and the laser driver ampli-

fiers and will use existing OMEGA power-conditioning units with modern controls and new components. A new charging power supply will replace the 12-head chargers formerly used in the OMEGA units. These PCU's will not have PILC circuits and will store a maximum of 78 kJ at 7.5 kV. The second type of rod PCU will be used for the A, B, and C stages of rod amplifiers. These are basically a cross between the disk amplifier PCU and the stage-D rod amplifier PCU. These totally new units will also store 78 kJ at 7.5 kV (maximum voltage) and will have PILC circuits similar to the disk amplifiers.

All PCU's will require a timing signal to synchronize firing of the amplifiers. This signal will originate in the master timing system (located in the pulse-generation room) and be distributed throughout the capacitor bays to each PCU. The initiation of this signal is commanded by the power-conditioning control computer. This signal will be delayed individually at each PCU by an amount set by the power-conditioning control computer. This delay is adjusted to synchronize the peak of the amplifier gain to the arrival of the laser pulse at that amplifier. The performance of the power-conditioning system is outlined in Table 57.I.

**Upgrade Control System**

The Upgrade Control System (UCS) will provide operators with remote control of subsystems, displays of sensor data, and safe, automatic sequencing of key processes. The control system will also collect and record information about each shot.

**1. Control System Functions**

The following eight functions have been assigned to the UCS as the design of the OMEGA Upgrade system has progressed:

Table 57.I: PFN Specifications

	Disk Amps	Rod Amps
Pulse width ( $\mu$ s)	550	475
Linear resistance (m $\Omega$ )	120	100
Inductance ( $\mu$ H)	180	55
Capacitance ( $\mu$ F)	210	460
Charging voltage (kV)	14.1	7.3
Stored energy/PFN (kJ)	20.9	12.3
Total energy (MJ)	35.1	7.1
<b>TOTAL ENERGY (MJ)</b>	<b>42.2</b>	

1. Control of the electric power and the fluid facilities that support the beamline amplifiers
2. Routine operational alignment of the beamline optics
3. Control of the laser drivers subsystem
4. Diagnosis of the laser system's performance
5. Control of personnel access to the laser bay, target bay, capacitor bays, and the rooms under the target bay
6. Control of the vacuum system that services the spatial filters
7. Control and, where appropriate, data-acquisition support of the instruments that sense shot-event parameters
8. Control of the vacuum systems that service the target chamber and the target diagnostic instruments

eration and data-acquisition functions of the instruments that measure the characteristics of the laser pulse produced by the beamlines.

5. The facility interlock function will control personnel access and the main electric power source as a function of system status.
6. The experimental system function will control the target chamber subsystems and the data-acquisition systems for the target diagnostic instruments.

An additional **seventh function**, the shot executive, is also required. This function will serve to coordinate the activities of the other functions when it is necessary for them to work together to conduct a target shot.

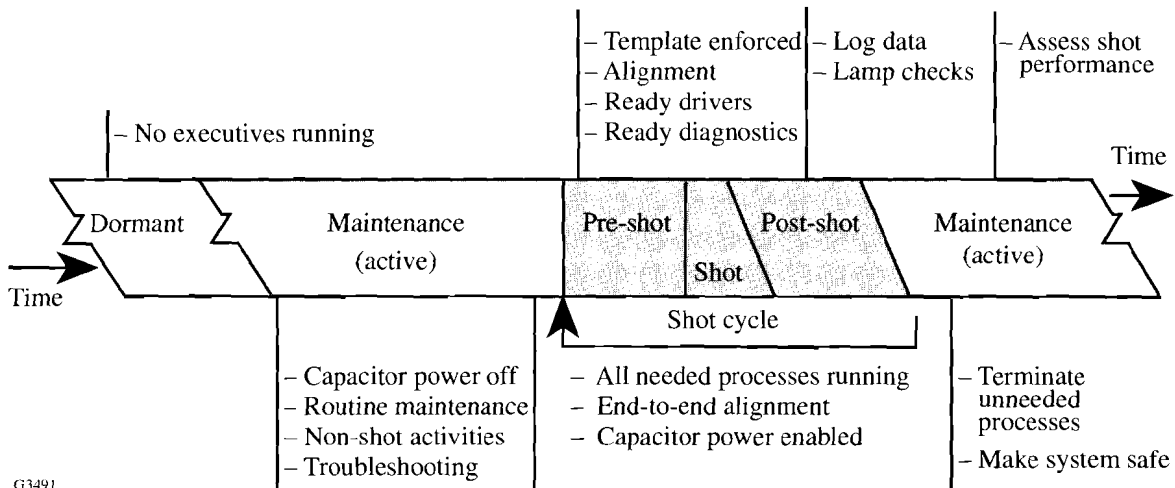
These have been allocated to six top-to-bottom "functions" within the UCS:

1. The power-conditioning function will provide the power conditioning and fluid control for all of the single-pass amplifiers in the system, including those in the laser drivers subsystem.
2. The alignment function will implement beamline alignment processes, beamline energy control, and beam-to-beam timing control.
3. The laser drivers function will provide control and monitoring of the initial pulse generation and amplification processes. This includes the multipass lasers at the start of the system and the appropriate alignment and beam diagnostic elements.
4. The beamline diagnostics function will control the op-

2. Operations Timing

The activities that make up these functions take place during the operational periods that precede and follow the brief high-energy shot event. (Figure 57.16 illustrates this relationship.) The control system activities support maintaining the system, preparing it for the shot, and recording the shot results. The timing resolution necessary to implement these requirements is of the order of tens of seconds.

The shot executive function initiates the "pre-shot" processes that must take place in the hour before a shot, verifies that the other functions are ready for the actual shot, and initiates the "shot" preparations. Thereafter, the power-conditioning function controls the laser system to within ten seconds of the shot and then enables the key system elements to



G3491

Figure 57.16

The flow (in time) of the system control operation for routine shots and maintenance. When the capacitor power supply is enabled, the system is termed active. The shot cycle is a heightened readiness state involving all of the control functions.

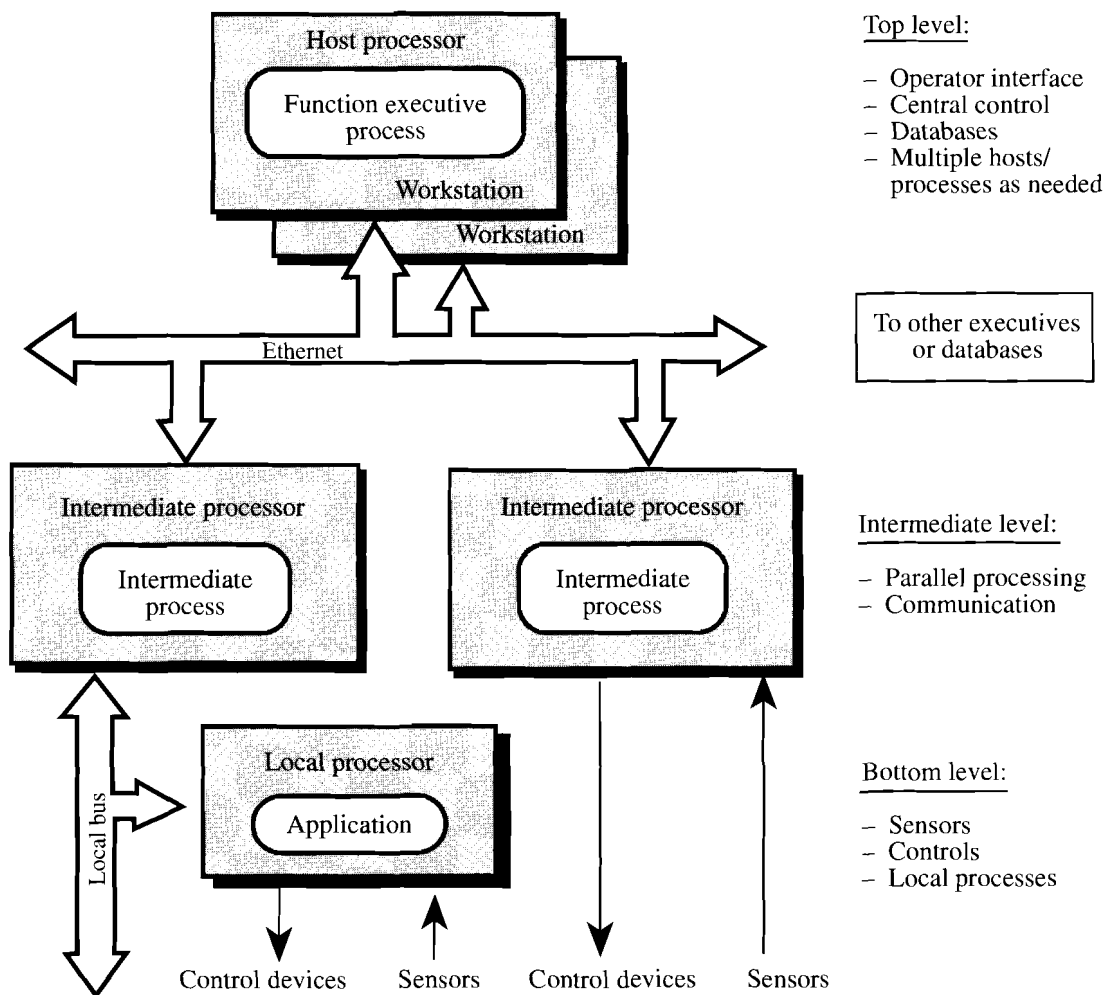
proceed on the basis of the electrical master timing signal. The events synchronized by the master signal include generation of the optical pulses in the laser drivers subsystem, the electrical pulses that drive the flash lamps in the laser amplifiers, and the operation of diagnostic instruments. The timing and duration requirements for the flash-lamp current are in the 100- $\mu$ s range and are implemented by the electronic circuits in the PFN's. The submicrosecond characteristics of the optical pulses are achieved by electro-optical techniques.

### 3. General Architecture

The general hardware/software architecture that will implement each of these functions is illustrated in Fig. 57.17. Separate "executive" processes for each function will run on

workstations installed in the control room. These are referred to as "host processors" and will be connected to each other and to other OMEGA Upgrade system computers via a dedicated Ethernet local area network.

Each function's executive process will provide the operator interface for the function and will exert control over and receive information from devices in the bays by communicating with one or more "intermediate" processors over the Ethernet. These intermediate computers serve to relieve the executive of routine computation and downward communication tasks. Communication between the executive processes is necessary primarily for coordination of shot-related events.



G3492

Figure 57.17 The top-level architecture of the OMEGA Upgrade control system. Three levels of computers are used to provide a system with distributed intelligence. Personnel interact with a host processor, which commands, via two local networks, numerous microprocessor-controlled devices.

At least two variations of the intermediate and bottom architectural levels will be employed in the UCS. In many situations, a third layer of computer control based on a Neuron<sup>®</sup> Device Control will be used. The Neuron is an inexpensive, single-chip, multiprocessor system that implements a local area network protocol called a local operating network (LON) and provides for control of devices and acquisition and communication of data. In the UCS, nearly 2000 Neurons will be used to integrate simple control actuators and feedback sensors under software control to produce more-sophisticated, local control devices. Neurons will also be used to acquire and digitize data from diagnostic sensors. Where the Neurons are used, the primary function of the intermediate process is to act as interpreter between the Ethernet and the LON. In this case the intermediate processor is called a LON Ethernet Network Adapter (LENA). Each LENA will service four LON's (channels), each of which will support 50 to 150 Neurons. (This configuration is illustrated on the left side of Fig. 57.17.)

Another architectural variation (illustrated on the right side of Fig. 57.17) is used to control the alignment video cameras and to acquire and process video frame data. This configuration is referred to as a digital expandable still camera (DESC). Here the intermediate process controls up to five cameras directly, rather than via a network. The DESC process also performs the digital image processing necessary to convert frames of video data into two-axis error data that is transmitted to the alignment function executive process. Similar configurations will be used to control diagnostic devices in the laser drivers, laser diagnostics, and experimental system functions.

#### 4. Facility Interlocks

Personnel safety is of primary importance in the design of the OMEGA Upgrade System. Three major classes of hazards are addressed at a fundamental level by interlock functions built into the utilities that are part of the laboratory facility supporting the laser system. These are

- control of the power source for the high voltages inherent in the laser amplifiers;
- control of the warnings issued when the presence of alignment laser emissions could constitute an eye hazard; and
- active and passive monitoring of the location of personnel in the bays.

These and other basic facility-monitoring features are included in the following specific facility interlock subsystems:

- The electric power source for all the laser amplifiers is a commercial power substation formally designated Unit Substation #2 and commonly referred to as "the 750-kVA power source." This equipment is located at the west end of Capacitor Bay 1 on the lower level of the slab. No electric power will be available to the power-conditioning units unless a relay in the substation is closed by logic built into facility interlock hardware.
- Five laser sources and 79 beam-train shutters will be monitored to control lighted warning signs at seven locations. A voice enunciator will provide audible warnings of status changes.
- Approximately 30 surveillance video cameras will provide operators with views of the bays.
- Approximately 44 passive infrared motion sensors will alert operators to movements at times when there should be no activity.
- The open/closed status of 28 doors will be remotely sensed and monitored; 16 of these doors will also be equipped with remotely controlled locks.
- During normal operations, the identity of the occupants in each of five controlled zones will be monitored by means of a combination of badge readers and door-lock controls at the entrances.
- Bells and light beacons will warn of impending capacitor charging.
- Manual "dump buttons" are provided at numerous locations in the bays. These will directly disable the 750-kVA power and short-circuit all of the high-voltage capacitors in the system.
- The interlock logic will control grounding isolation features that ensure both personnel safety for routine operations and hardware safety during the shot events.
- The interlock logic will be able to override other controls and turn off the bay lighting.

## 5. Beamline Diagnostics

Acquisition of beamline diagnostic data is a major branch of the overall Upgrade control system architecture. One of the five control system executive workstations (beamline diagnostic executive) is dedicated to operating the laser diagnostics configured on the 60 beamlines located in the laser bay. These diagnostics include the following measurement systems:

- Harmonic energy detection (IR, green, and UV energy measurements)
- Full-aperture, high-flux calorimeters
- Beamline-to-beamline IR energy balance (splitting ratios, wave-plate settings)
- UV-on-target energy transport ( $3\omega$  to target, beam-balance compensation)

At the highest level of the control architecture, the executive workstation first issues commands to the acquisition subsystems and then collects and processes the data for the laser system operators to evaluate. Below the executive workstation in this hierarchy are the local data-acquisition nodes that contain the specialized hardware used to interface to the laser diagnostics. These nodes reside on a combination of Versa Module Europa (VME) and Computer Automated Measurement and Control (CAMAC) platforms, depending on the application. In either case, these nodes communicate with the executive workstations through an Ethernet link. The local data-acquisition VME platform nodes contain embedded SPARC computers. These computers handle the lower-level input/output control and acquisition sequencing required to collect diagnostic data. The CAMAC platforms are interfaced to the VME platforms through high-speed,  $\sim 1.5$ -Mb/s bus adapters and have no local intelligence. This interface allows data to flow from CAMAC into the VME system at, or near, CAMAC backplane speeds. At the lowest level of the acquisition architecture are transient digitizing oscilloscopes and CCD (charge coupled device) camera arrays, discrete photodiodes, etc. These are used to capture electrical waveforms, two-dimensional optical data, pulsed events, etc. The oscilloscopes are interfaced to the intelligent VME nodes through dedicated general purpose interface bus (GPIB) communication lines. The CCD cameras have local video controllers and digitizing frame grabbers to buffer the images before uploading the data to the executive workstations.

Diagnosis and adjustment of the beam arrival time at the target is another critical control-system function. The responsibility for the associated tasks is shared by two of the top-level control-system functions. The beam arrival times will be measured using a photodiode at the target location and an rf interferometric technique. This system will determine the time differential between the arrival of a laser pulse at that location and the arrival of the same pulse at a reference location. The laser pulses will originate at the IR alignment table (IRAT) and be propagated through the beamlines from the stage-A splitter to the target chamber. The arrival time for each of the 60 beams is acquired sequentially. The resolution of the measurement is expected to be better than 1.5 ps.

This process must be performed as a special activity separate from normal shot operations. The alignment function will configure the IRAT and the beamlines to provide the pulses to the photodiode sensors. The experimental system function will position and control the sensor at the target location and acquire/reduce the time-differential data. The alignment function will process the timing data to determine the path adjustments required and then control the path length adjustment systems (PLAS's) to implement any required changes.

## Optomechanical Systems

### 1. Optical System Design

The optical design of the system was constrained primarily by two factors: the need to fit the upgraded laser into the existing building and the desire to reuse as much hardware as possible (spatial filters, in particular). The top-level requirements for the total energy and the number of beams dictated the amplifier staging and the beam splitting required. Optical damage thresholds dictated the minimum beam diameters in each stage, which in turn fixed the magnification between stages. From these baselines the system was designed to incorporate image relaying as required by the implementation of SSD (smoothing by spectral dispersion) and by sound laser design practices.

Given the above, the layout of the laser system was then refined to ensure that no damage occurs from "ghost" reflections, provide equal path lengths in all beamlines, and provide an accessible and manageable system. The configuration has undergone several changes since the preliminary design. These changes were dictated by performance issues and ultimately resulted in a simpler configuration.

Once the system configuration was determined, error budgets were performed for energy, wavefront, alignment, and polarization. Each of these budgets was then distributed to the individual components in the system to formulate the requirements. For example, the wavefront budget was used to specify that the wavefront error contributed by each optical component not exceed  $\lambda/10$ . This value is relatively small because the disk amplifiers consume a major portion of the error budget. The pointing error in the system is driven by the requirement to point beams onto target with a precision of  $\sim 5\%$  of the target radius. Given a minimum target radius of  $300\ \mu\text{m}$  and a 1.8-m-focal-length final lens, the total pointing error budget is  $8.33\ \mu\text{rad}$ . The distribution of this error affected the design of the alignment sensor packages, the optical mounts, and the various structures supporting the laser. It was this pointing error budget that necessitated the implementation of the epoxy/granite structures for the stage-F alignment sensor packages (ASP's), which act as the optical alignment references for the system.

The energy budget specified the fluences at various points in the system, thereby impacting the choice of substrate material, typically BK-7 or fused silica. The energy-balance constraints drove a requirement for identical beam sizes at all the frequency-conversion cells, to match the intensity and hence the conversion efficiency. This requirement forced a tight specification ( $\pm 0.5\%$ ) for the focal length of the spatial filter lens. About that absolute specification, all lenses of a given type are corrected during fabrication such that all focal lengths are matched to  $\pm 0.2\%$ .

The polarization budget suggested the contrast of the polarization required for efficient splitting and amplification. The requirements for balanced beam-to-beam frequency conversion dictated the need for Brewster-angle polarizers ahead of the FCC's. Because of the precision needed, these are required in spite of the (50:1) polarization contrast the Brewster-angle disk amplifiers provide at the end of the amplifier stages. The disk amplifiers provide a relative insensitivity to depolarization early in the system.

The resultant design is a system that fits into the existing building and maximizes the use of equipment from OMEGA. (Over 90% of existing OMEGA spatial filters were used in the upgraded system.) The system includes path-length adjustments that can provide simultaneous arrival of beam pulses at the target to within  $\pm 3\ \text{ps}$ . Individual beams can be intentionally mistimed to  $\pm 5\ \text{ns}$  with respect to  $t = 0$ . Mapping the

UV beams to the spherical target chamber was performed to minimize the sensitivity to variations in performance of the individual amplifiers. This mapping (discussed under *Target Area*) uses two mirrors per beam, ensures that incident angles on the mirrors are less than  $60^\circ$ , maintains equal path lengths from the FCC's to the target, and fits within the existing space. The system design will deliver beams with sufficient energy, quality, and alignment accuracy to attain the ultimate goal of 1%–2% nonuniformity on target.

## 2. Optical Components

Optical components for the OMEGA Upgrade are being procured through several major contracts with five leading optical fabrication vendors. This section summarizes the engineering effort that led to these components being specified and purchased (at budget), with their performance meeting Upgrade requirements.

The top-level requirements for the laser performance and uniformity dictated an array of lesser requirements for appropriate beam profiles and energy levels at the target while minimizing fluences throughout the chain that could potentially damage optical components. From the requirements and configuration constraints, computer simulations of beam transport allowed determination of such parameters as fluence, B-integral, allowable wavefront and alignment error, and the required power balance.

Once the on-target error allowances were determined, optical engineers statistically apportioned the error among the components in the system. Budgets were made for the various types of error and used to establish surface finish and transmitted wavefront tolerances for each optical component. Once the fluences in the system were known, the optical material for each component could be chosen. The choice was typically between BK-7 for fluences below  $2.0\ \text{J}/\text{cm}^2$  and fused silica for fluences above that.

Compilations of these parameters resulted in a specification control drawing (SCD) and statement of work (SOW) for each type of optical component in the Upgrade. These documents served as the basis for quotation requests from the optics vendors and as the measure of achievement for contractual obligations.

Specifications were written for the following categories of optical components:

- Spatial filter lenses
- Mirrors and beamsplitters
- Polarization control optics
- Aspheric focus lenses
- ASP optical components

The procurement cycle for each of these components required the vendor to generate plans for manufacturing, processing, cleaning, and testing of each component prior to the start of manufacturing. Source inspection, or at a minimum examination of vendor test data, has ensured that all optical components meet specifications. Typical specifications for these components (all measured at 1054 nm) are

transmitted wavefront error:  $\pm 1/10$  wave  
 flatness (mirrors):  $\pm 1/20$  wave  
 surface roughness:  $< 10 \text{ \AA}$  (rms)

### 3. Optical Coatings

The requirements for the OMEGA Upgrade optical coatings are discussed in the Preliminary Design Document<sup>1</sup> and in detail in the Optics Coating Requirements document.<sup>2</sup> The development of Upgrade coatings, in general, and the transport mirror coating, in particular, is described in several reports in the LLE Review.<sup>3,4</sup> A coating specification<sup>5</sup> also outlines the required tests and inspection criteria for all coated optics. A summary of the coating requirements is given in Table 57.II. The coating designations in the left column of this chart are discussed below. All the coatings have been designed, fabricated onto prototype substrates, and tested for both optical and damage specifications.

a. IR coatings. The coatings used in the IR (1054-nm) portion of the laser system comprise antireflection and reflector coatings. The substrates for the antireflection coatings are either BK-7 glass or fused silica depending on the incident fluence. The BK-7 substrates receive a vacuum-evaporated dielectric coating using an yttrium-oxide/silicon-dioxide design (1 $\omega$ AR, 1 $\omega$ AR45), while the fused silica optics are coated

Table 57.II: Coating Requirements for the OMEGA Upgrade.

Coating Designation	LC Gap	Wavelength	Incident Angle	Control Value	Reflectance		Transmittance		Max. Fluence* (J/cm <sup>2</sup> )	
					S%	P%	P%	P/S		
1 $\omega$ HRSP45	6.5 $\mu$ 13 $\mu$ >18 $\mu$	1054 nm	45°	R	99.5	>99.5	>96		5.4	
1 $\omega$ RSTP45		1054 nm	45°	R	>99.5	<4.0				5.4
1 $\omega$ 99RS45		1054 nm	45°	R	99 $\pm$ 0.5					5.4
1 $\omega$ 99RP45		1054 nm	45°	R	99 $\pm$ 0.5				4.5	
1 $\omega$ StressAR		1054 nm	45°	R	<1.0	<0.5			5.4	
1 $\omega$ AR		1054 nm	0	R	<0.5	<0.5			5.6	
1 $\omega$ RSTP57		1054 nm	57°	T			95	500/1	5.1	
1 $\omega$ AR45		1054 nm	45°	R	<1.0	<0.5			5.4	
LCS6.5		No Optical Requirements								
LCS6.5										
LCS9										
1 $\omega$ ARALIGN			1054 nm	0	R	<1.0	<1.0			2.9
			351 nm	0	R	>10	>10			2.9
SG1/2 $\omega$ AR		703 nm (cwl)	0	R	<1.0	<1.0			2.9	
SG1 $\omega$ AR		1054 nm	0	R	<0.5	<0.5			5.4	
SG3 $\omega$ AR		351 nm	0	R	<0.5	<0.5			2.9	
SG3 $\omega$ AR/DPP		351 nm	0	R	<0.5	<0.5			3.6	
SG3/1 $\omega$ AR		351 nm/1054	0°-8°	R	<0.5	<0.5			3.6	
3 $\omega$ HRSP(ANG)		351 nm	0°-60°	R	>99.5	>99.5			2.9	
3 $\omega$ Stress		No Optical Requirements								
1/2/3 $\omega$ AR		351/527/1054	0	R	>85	>85			low power	

cwl = center wavelength

\*Note: Fluences assume 7-ns foot (F) pulse and 1.1-ns main (M) pulse.



with a porous-silica sol-gel (SG1 $\omega$ AR). This high-damage-threshold (but delicate) coating was chosen on the basis of the fluence levels at the optics. The design may be modified after some experience on the glass development laser. The reflector coatings include high-reflectivity mirrors, partial reflectors, 45°-incidence polarizing beamsplitters, and 57°-incidence polarizers. These coatings are all based on a vacuum-evaporated dielectric coating using tantalum-oxide/silicon-dioxide designs. These materials have been extensively developed for high damage threshold and optical performance.

During initial manufacture of the reflector coating, stresses from the coating deformed the optic, causing these optics to fail optical surface figure testing. After several remedies were investigated, it was discovered that the best solution is a coating (1 $\omega$ StressAR) that when applied to the back side of the optics produces similar stresses. This rear-side coating will be applied to all substrates coated with dielectric multilayers.

A coating process was developed to produce spacers of evaporated material for the liquid crystal devices in the system. These spacers provide better control of wedge tolerance (1.5 arc/s) in the assembled device, more accurate thickness of the liquid crystal layer (6.5  $\mu\text{m} \pm 0.5 \mu\text{m}$ ), and faster assembly methods than the mylar spacers previously used.

The coating for the frequency-conversion crystals is a single-layer sol-gel design for the three wavelengths (SG1 $\omega$ AR, SG1/2 $\omega$ AR, and SG3 $\omega$ AR). When applying these coatings, much of the effort is in the tooling and process development required for the dipping and spinning deposition processes. New polishing methods under consideration for these components also require developing cleaning methods to remove polishing oils.

**b. UV optics.** The UV (351-nm) transport optics are coated with a sol-gel antireflection coating (SG3 $\omega$ AR) for the transmissive optics and a high-reflector coating [3 $\omega$ HRSP(ANG)] for the transport mirrors. These sol-gel coatings have been designed, developed, and tested, and the production processes have been determined for all optics. For each application, the composition and design of the coatings will vary depending on the incidence angle of the beam and the orientation of the electric vector with respect to the coated surface. Optics having a low incidence angle and predominantly *s*-polarized light will use a design based on hafnium oxide/silicon dioxide. Optics that combine high incidence angle and predominately *p*-polarized light use a design containing more costly scan-

dium-oxide/silicon-dioxide coatings. For a given angle, each design will provide the specified reflectance with the minimum number of layers to improve damage characteristics. These designs will also be modified to reduce the time-averaged electric field in the upper layers of the coatings.

A great deal of effort has gone into the design of the substrate cleaning and storage tooling, coating tooling, testing tooling, and handling tooling to ensure that no process degrades the high-quality substrate surfaces. Preliminary results from the newly installed 1.8-m coating chamber indicate that all uniformity requirements for the Upgrade optics will be met. A substantial effort went into establishing a sol-gel coating capability for the 650 optics to be coated as well as the facility needed to clean the 2000 optics for the Upgrade.

#### 4. Optomechanical Design

Four key design constraints drove the Upgrade's optomechanical design. The first was strain-free mounting of all optical components. The mounts generally consist of three-point, 6°-of-freedom, exact-constraint designs that prevent typical mount manufacturing, assembly, and environmental tolerances from distorting the precision optical components. The second key feature is precision pointing and centering control of optical components. These include fixed mounts, manual drives, and motorized drives that typically have microinch and/or microradian accuracy and stability requirements. The third constraint is to provide an adjustment range adequate to acquire the laser beam within the optic's clear aperture. The range must be sufficient to compensate for typical fabrication and structure installation tolerances. Finally, all optical components must be packaged within the space constraints allocated by the 60-beam OMEGA Upgrade configuration. Examples of Upgrade optomechanical designs are the periscope mirror assembly (PMA), focus lens assembly (FLAS), transport mirror mount, spatial filters, and path length adjustment system (PLAS).

#### 5. System Alignment

The alignment of the beamline segments is performed using an IR cw alignment laser and various references (typically crosshairs) located throughout the system. These references define the beam path upon which the laser system components are located. Once the system is aligned, the alignment beam propagates through the system and defines the location and direction the pulsed beam will travel during a shot. All of the optical components in the IR system are installed and aligned using this alignment beam.

End-to-end alignment of a frequency-tripled, IR laser system such as OMEGA presents a difficult alignment problem because the relatively low-power, cw IR alignment laser will not be converted to UV by the conversion crystals. This, along with the low IR reflectivity of the Upgrade's UV transport mirrors, means that a single alignment beam cannot be used to align the system from source to target.

The Upgrade alignment system therefore uses two wavelengths, unlike the previous system that was aligned from the oscillator to the target using IR light. While two wavelengths increase the system complexity, they eliminate the two disadvantages of single-wavelength alignment: the transport mirrors no longer need dual-function (IR/UV) coatings (because UV light is used to align these optics), and the focus lenses will not have to be translated after IR alignment to compensate for chromatic shift. The former dramatically improves the damage threshold of the UV coating, and the latter improves the operational accuracy of alignment. The IR portion of the laser is aligned using a 1054-nm Nd:YLF laser, together with alignment sensor packages located at the driver and stages A, C, and F within each beamline. For alignment of the UV portion of the system, a full-aperture, 351-nm cw laser is injected into the beam after the FCC's and just before the omnichromatic F-ASP's. This is done with movable mirrors located in the target bay. Co-alignment of this injected beam to the IR pulsed beam is performed using the F-ASP. An alignment sensor package located on the UV alignment table (UVAT) measures the alignment of the injected UV beams.

**a. IR alignment.** The following basic processes will be necessary to routinely align the IR beamlines:

1. Laser drivers and IR alignment laser injection  
(1 beamline segment)
2. Stage A–C pointing and centering  
(15 beamline segments)
3. Stage C–F pointing and centering  
(60 beamline segments)

Each process involves five steps: setup, image analysis, action determination, action implementation, and confirmation.

Process 1 requires the alignment laser and driver to be aligned into the A-splitter area by using an alignment sensor package in the A splitter (A-ASP). The ASP has pointing and centering references to ensure that the beam entering the stage-A splitter has the correct direction and position to propa-

gate down the laser beamline. The driver injection is done after the alignment of the laser driver (not part of this procedure) and is necessary to propagate a driver beam into the laser chain. The backlighter driver is injected into the middle A–C segment and is aligned by the stage-A ASP. This injection is a somewhat manual process and is not part of the automated alignment routine. The following hardware is required: laser drivers, infrared alignment table (IRAT), and A-ASP.

Process 2, the alignment of the segment from the stage-A splitter to stage-C ASP, involves the alignment of the beams propagating from east to west in the laser bay and is performed using the alignment laser after it has been injected. This process is depicted in Fig. 57.18. Process 3 aligns the last portion of the IR system, the stage-C splitter to F-ASP, and is depicted in Fig. 57.19.

When all three sections are complete, the operator is assured that the centering reference at the end of the driver line has been transferred (within tolerances) to the centering fiducials at the F-ASP. This, coupled with the intermediate centering checks, ensures that the beam will not be vignetted on any optics in the laser chain. Similarly, the beam pointing in all stages is checked, corrected, and verified. The final IR pointing and centering positions are recorded by the F-ASP to be used as a reference for the UV alignment process.

**b. UV alignment.** The periscope mirror assembly (PMA) and the F-ASP are the major elements in the UV scheme. The PMA includes the UVAT and a system that positions a set of mirrors near the face of the shield wall in front of the F-ASP's. In each position, these mirrors form a periscope that injects a UV alignment beam, which originates in the UVAT, into one of the 60 beamlines at the input end of its F-ASP. After the UV beam is correctly aligned to the fiducial in the F-ASP, it is transmitted to the target chamber and retro-reflected to a video camera that is part of the UV-ASP on the UVAT. (The beam may also be transmitted back to the UVAT via the opposing beamline that has also been accessed by the PMA.) The video signal is processed to provide position-error data that is used to drive the motorized end-mirror and target-mirror mounts to correct the pointing and centering of the beam or to adjust the focus lens in the FLAS. The PMA mirrors are then repositioned to inject the alignment beam into another beamline.

The following basic processes will be necessary to routinely align the UV optical trains to correctly deliver the shot pulse to the target:

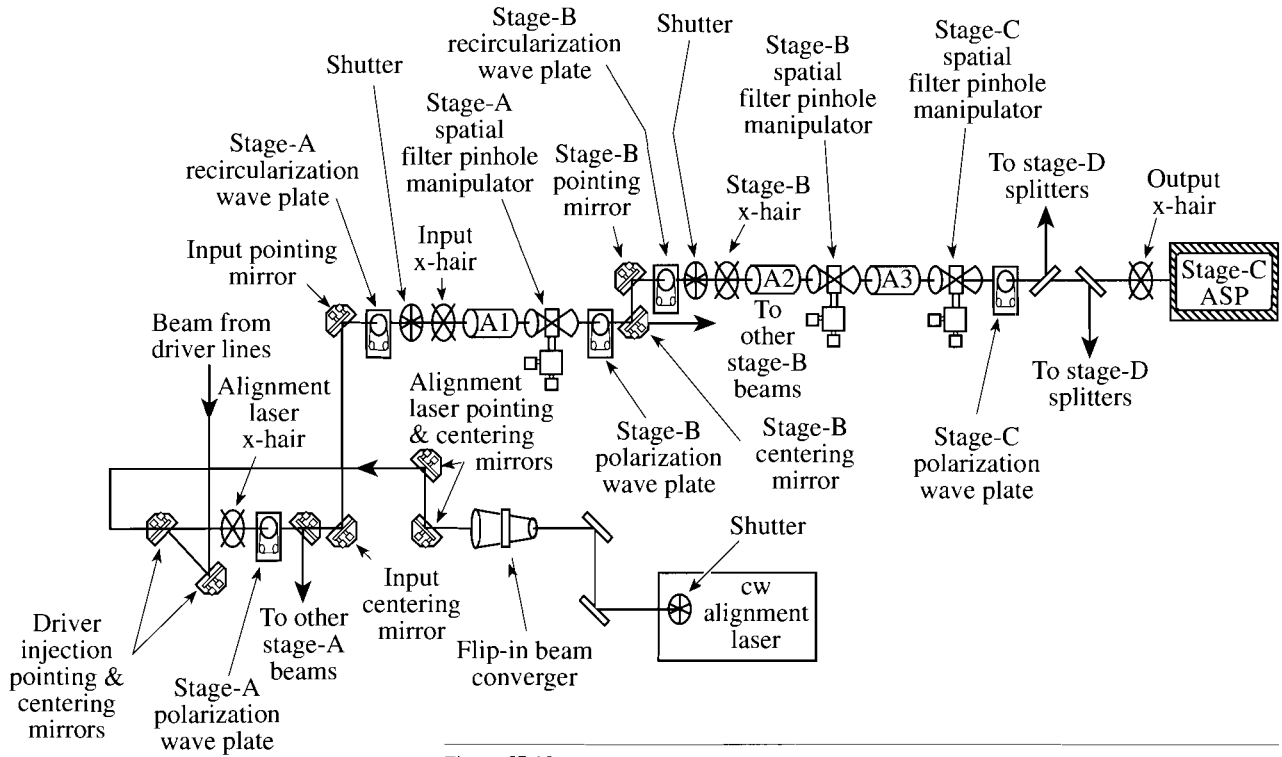


Figure 57.18  
The optomechanical devices in an OMEGA Upgrade beamline from the laser driver to stage C.

G3473

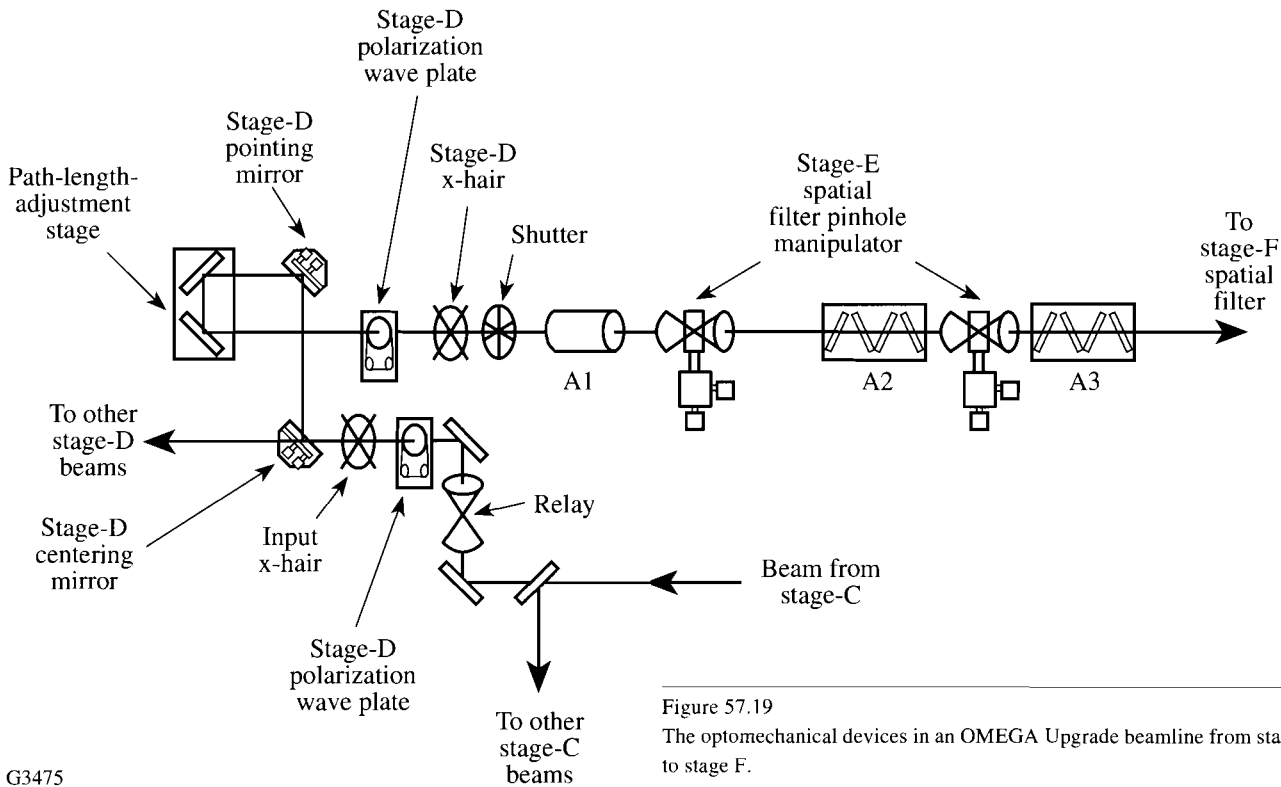


Figure 57.19  
The optomechanical devices in an OMEGA Upgrade beamline from stage C to stage F.

G3475

1. UVAT laser injection
2. UV transport system pointing and centering
3. Focusing

As with IR alignment, each process involves the five steps: setup, image analysis, action determination, action implementation, and confirmation. Here each process will be performed on the 60 separate beamlines, and the set-up step includes positioning and adjusting the PMA mirrors. Figure 57.20 depicts the optical configuration to perform alignment of the UV transport system. The UV alignment system will also be used to align the 60 FCC assemblies to their respective beamlines.

c. Propagation of centering errors. During the injection alignment, the alignment table and driver fiducials are centered on the system fiducial. In the A to C split alignment, the system fiducial is centered to the A fiducial and the A to the B fiducial.

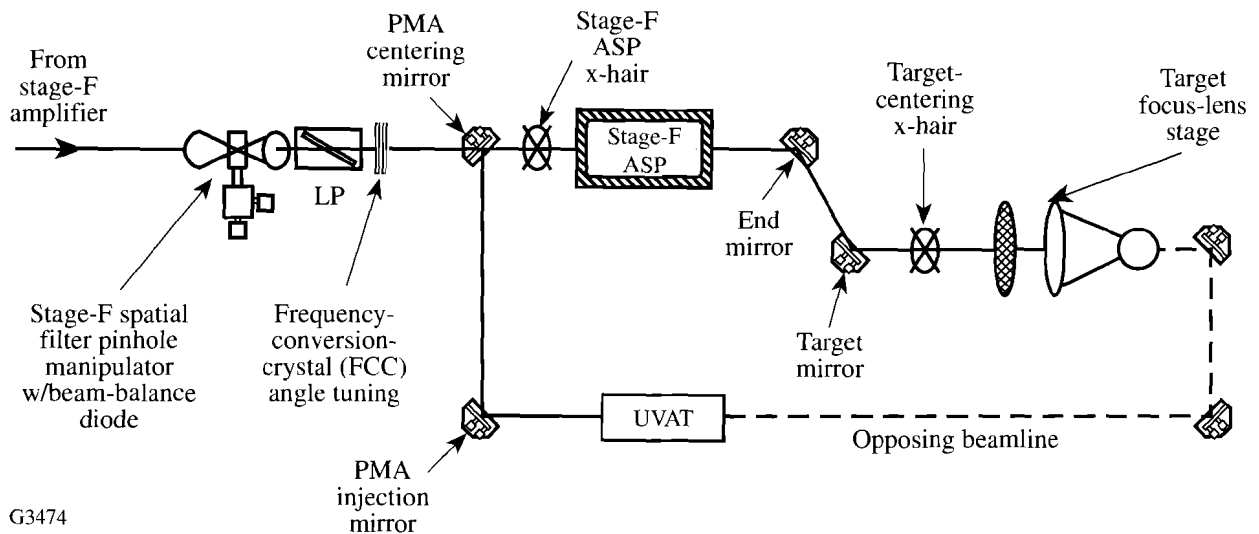
To minimize the accumulation of errors, the C split to F-ASP alignment will center the A-splitter fiducial to the D-splitter fiducial and confirm the A-splitter fiducial to the F-ASP fiducial for final IR centering.

The UV targeting will center the F-ASP fiducial to the target mirror fiducial creating a total of four stages where centering errors can occur: (1) driver to system, (2) system to

cluster, (3) cluster to PMA, and (4) PMA to target mirror. The first transfer is done so that the driver line is not used for beam alignment, and the injection need not be done at the C-ASP's. The second is necessary because the system fiducial is not at an image plane and cannot be expected to have sufficient image quality for alignment past the A-split. The third transfer is necessary because targeting cannot be done in the IR. The final transfer is used to center the target mirror and the FLAS.

Wherever possible, alignment will be performed in parallel steps across the beamlines to minimize the time needed to align the entire system. It is intended to utilize the parallel structure of the control network and the image processing to minimize the time required for each alignment step. The capability to align individual or subgroups of the beamlines is still required, even though it does not use the alignment hardware to its maximum efficiency.

d. Alignment sensor packages. The alignment sensor packages (ASP's) are stable optical telescopes used to view an alignment beam propagating in a laser beamline. They monitor the alignment stability of the system by sensing the pointing of the alignment lasers, and the position of the laser beam on optical components by sensing the position of alignment fiducials (e.g., crosshairs). These fiducials can be automatically inserted into the beamline or manually attached to optomechanical assemblies such as amplifiers and spatial filters. The ASP's are also used to view the position of the



G3474

Figure 57.20  
The optomechanical devices in an OMEGA Upgrade beamline from stage F to the target.

spatial filter (SF) pinholes to allow the automated alignment system to center the SF pinholes onto the beam.

The ASP's are the primary sensors for the beamline alignment system and typically reside at the ends of the beamline segments. Each ASP contains a solid-state image sensor (CCD) to view either the focus of the telescope objective (beam pointing) or the output image of the telescope, which shows the position of alignment fiducials (beam centering). Two-state devices move components within the ASP's to allow either of these functions to be performed by a single image sensor. The ASP's contain no moving or adjustable components between the entrance pupil and the point where the beam focuses on an alignment reticle. This feature provides long-term stability of the pointing reference for the beam.

To establish and maintain the beam path, the ASP's are used to view flip-in fiducials (FIF's) at the start and end of each beamline. These FIF's are surveyed into place during laser system construction and then become the reference for subsequent alignments. The ASP's locate the end fiducial relative to the image of the start fiducial to monitor beamline centering stability and maintain the beamline geometry of the laser system. Misalignments are corrected using mirrors located just before the start fiducials.

Four sets of ASP's are employed in the OMEGA laser system. A single-driver ASP resides at the end of the laser driver. A single stage-A ASP resides within the stage-A splitter. Fifteen stage-C ASP's reside at the end of the 15 beamlines that run from the B splitter to the C splitter. Sixty stage-F ASP's reside at the end of the 60 beamlines that run from the D splitter through to the FCC's. These four sets are made up of two basic types of ASP's: the driver, stage-A, and stage-C ASP's are nearly identical; the stage-F ASP is significantly different.

The driver, stage-A, and stage-C ASP's are all existing OMEGA beam diagnostic packages (BDP's) modified to sense pointing and centering with a single, solid-state detector. The top-level performance requirements for the driver, A, and C alignment sensor packages were derived from the pointing error budget, which dictated the pointing sensitivity, short-term stability, and long-term stability (drift) for these instruments. Where possible, the requirements for the driver, A-, and C-ASP's were made similar to allow common modifications to the existing BDP's and to minimize design time.

The primary function of the driver ASP is to monitor the driver alignment, particularly the coalignment of the foot and main pulses. The driver ASP must sense pointing to  $1.3\text{-}\mu\text{rad}$  accuracy over a 10-mrad field of view.

The stage-A ASP monitors the injection of the driver line and IRAT beams into the laser system. It is mounted in the stage-A splitter structure and is also designed to sense pointing to  $1.3\text{ }\mu\text{rad}$  over a 10-mrad field of view. This sensor must be able to diagnose beam centering (FIF position) to 0.13-mm accuracy and includes a collimation sensor to allow the collimation of the IRAT, foot-, and main-pulse drivers to be matched. This is important for the optical design (i.e., all three beams come to a common focus at the SF pinholes and at the target) as well as to maintain optimal frequency-conversion efficiency for the foot and main pulses.

The stage-C ASP monitors the alignment of the beamline segments from the B splitter to the C splitter. The stage-C ASP also must sense pointing to  $1\text{ }\mu\text{rad}$  over a 10-mrad field of view and must diagnose beam centering (FIF position) and drift to 0.19-mm accuracy.

The requirements for the stage-F ASP were derived from the pointing-error budget—a systematic, top-down, allocation of the top-level pointing error of  $8.33\text{ }\mu\text{rad}$  to the various components of the laser system. The driving considerations were for alignment precision ( $< 0.3\text{ }\mu\text{rad}$ ) and pointing stability ( $< 2.7\text{ }\mu\text{rad/h}$ ). The instrument is required to meet all three of these specifications. It was also required that the F-ASP use a bare glass reflection rather than transmission through a “leaky mirror” to minimize polarization effects and maximize radiometric stability.

The precision requirement led to the choice of an effective focal length of the F-ASP objective matched to the pixel size of the detector. This, in combination with the requirement for complete absence of chromatic aberration, led to the selection of a three-mirror, off-axis, all-reflective telescope for the F-ASP objective. Although the use of a reflective telescope puts more stringent requirements on the angular stability of the optomechanical system than a refractive system would, this is compensated by the complete lack of chromatic variation of optical performance provided by an all-reflective system.

The pointing stability requirement drove the mechanical design. In general, the requirement for extreme angular stabil-

ity leads the mechanical designer to strive for symmetry in all possible aspects of the mechanical structure. The beam-to-beam spacing caused adjacent F-ASP's to be nested together in such a fashion that individual one-beam instruments would, necessarily, have been highly asymmetrical. To avoid this, ten-beam F-ASP units were designed with modular subassemblies that can be removed for off-line service as required. To further improve the stability of these instruments, the main structure was made of Harcrete™, a cast epoxy/rock composite. This material's properties include high stiffness, low thermal conductivity, excellent vibration damping, excellent dimensional stability, and the ability to be cast into complex shapes. Figure 57.21 depicts two of the cast monoliths; the one on the right is sectioned to show the optic in a single F-ASP unit. Figure 57.22 shows in detail the beam paths through one of the F-ASP's.

To avoid the problem of post-adjustment drift, the critical optical mounts were designed to be nonadjustable. Adjustable installation fixtures permit the optics to be positioned correctly and then epoxied into place, using special low-shrinkage, high-stability epoxy. The installation fixtures are then removed from the F-ASP. This scheme provides the advantages of adjustability without the associated drift problems.

The moving parts of the F-ASP are components of modular subassemblies that can be removed for off-line service. The video camera, expected to be the least reliable component of the instrument, is contained in the relay subassembly, which mounts kinematically to the F-ASP. An off-line alignment fixture adjusts and tests the relay so that it will be correctly focused and aligned when inserted into the F-ASP structure.

## 6. Spatial Filters

Evacuated spatial filters are used after every amplifier stage in the OMEGA Upgrade to provide image relaying and various amounts of magnification. The filter sizes depend on the beam aperture and magnification; for instance, the stage-A filter is  $f/50$  and 5.6 m long, and the stage-F is  $f/22$  and 10.25 m long. Aspheric lenses are used in all the large-aperture spatial filters, thereby reducing the accumulated spherical error in the system.

The spatial filters comprise five subsections: the tube weldments, the lens cells, the lens spacers, the interface package, and the pinhole manipulator. The tube weldments are 316-stainless-steel tubes with flanges and are rated for

$5 \times 10^{-6}$  Torr. The nominal operation pressure for the spatial filters is 2 mTorr.

The lens cells and lens spacers are mounted on each end of the weldments. The cells are one-piece annular mounts for the lens and contain two O-ring grooves for vacuum seals, one on the spacer side and the other on the lens side. The cell contains a simple, spring-loaded retainer for the lens to facilitate installation and replacement. The lens spacer is an annular aluminum cylinder used to compensate for variations in the focal length of the lenses and manufacturing tolerances of the tube weldments. Custom sizing of each spacer for a specific tube and lens pair allows the collimation of each spatial filter to be strictly maintained. The length of the spacers will be determined to  $\leq 125 \mu\text{m}$  using a special fixture and collimation detector, thereby providing collimation of each spatial filter to  $\lambda/4$  @ 1.054 nm.

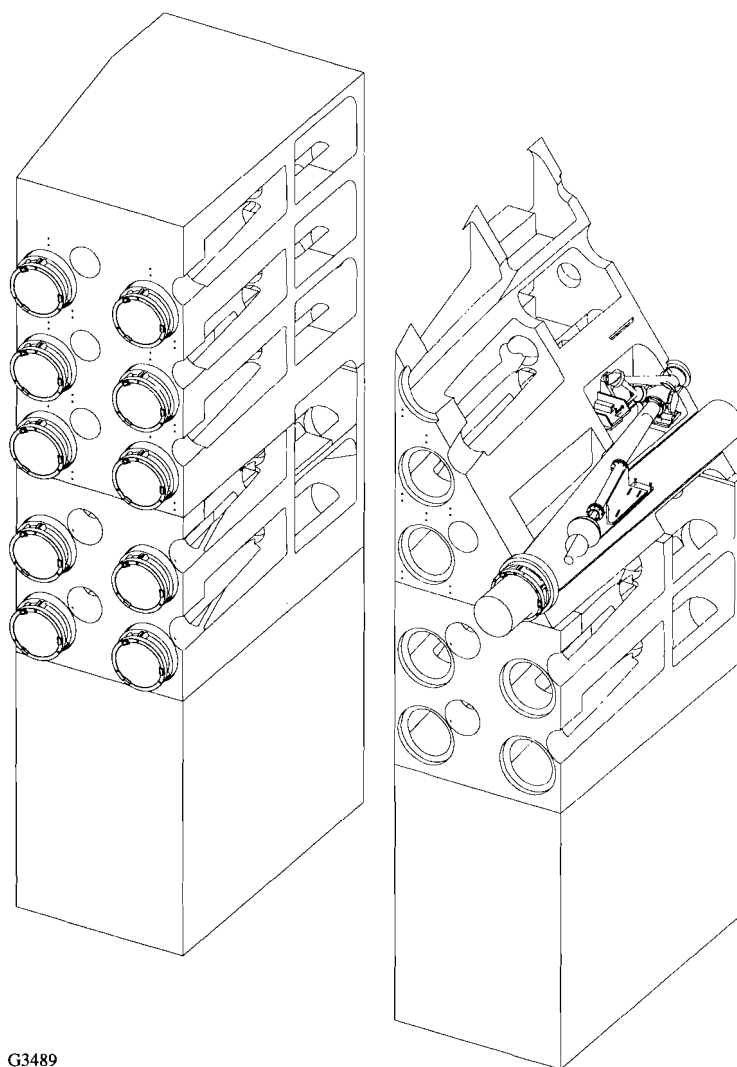
The pinhole manipulator positions the pinhole directly at the focal point of the spatial filter, requiring adjustment in three dimensions. The pinhole manipulators from the original OMEGA system will be used on the Upgrade for stages A–D. The size and close proximity of the stage-E and F spatial filters require a new manipulator that has the slides and motors located within the spatial filter tube. The mechanical and electrical components of these manipulators are vacuum compatible.

The interface between the spatial filter and the support structure will be an air bearing that will allow the entire filter to be moved out of the beam. This will allow for the necessary removal of the spatial filters during routine alignment; quick-disconnect pneumatic fittings will make this task easier.

## 7. Frequency Conversion Cells

The frequency-conversion crystals (FCC's) convert the fundamental wavelength of the OMEGA laser (1054 nm) to the second- (527-nm) and third- (351-nm) harmonic wavelengths. The frequency-conversion cells have been engineered to meet the requirements established in the OMEGA Upgrade Preliminary Design Document.<sup>1</sup> The following describes the engineering process that led to contracts with vendors capable of supplying high-quality, frequency-conversion components.

The parameters that contribute to uniform frequency conversion were established using simulations conducted by the



G3489

Figure 57.21  
Two of the monoliths for the stage-F alignment sensor package (F-ASP), each containing ten beamlines. A section through the right structure depicts the layout of the optics for a single beamline.

code “MIXER.”<sup>6</sup> To keep losses below 0.5% of the conversion efficiency at the peak of the main pulse, where the crystals are the most sensitive to errors, the following tolerances (obtained from Table 7.4 of Ref. 1 with adjustment where appropriate by the crystal thickness ratio 12:7.6) must be achieved:

Doubler misalignment	142 $\mu$ rad
Doubler wavelength shift	7 $\text{\AA}$
Doubler temperature	0.6°C
Tripler misalignment	29 $\mu$ rad
Tripler wavelength shift	0.2 $\text{\AA}$

Tripler temperature	0.1°C
Polarization angle	$\pm 0.3^\circ$
Fraction in wrong polarization	$3 \times 10^{-5}$

In the preliminary design, the doubling and tripling stages each used a thicker central crystal for efficient conversion of the foot pulse surrounded by a thinner, annular crystal for efficient conversion of the main pulse. During the detailed design, a thorough investigation and reevaluation of the required pulse shapes and the associated intensity distributions at the plane of the conversion crystals led to the selection of a single-thickness crystal, which efficiently converts both main

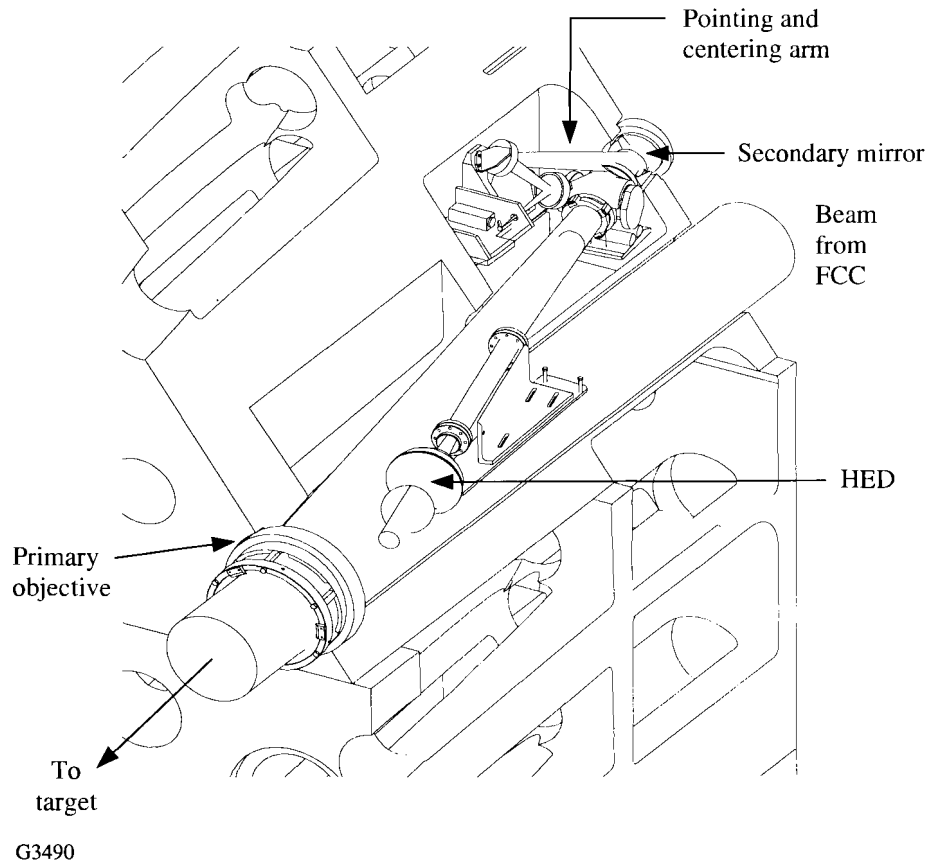


Figure 57.22  
Major optical components in a stage-F alignment sensor package (F-ASP) for a single beamline.

and foot pulses and maintains the same operating parameters. This design utilizes 12-mm-thick crystals (30-cm diam) for both the doubler and tripler.

Once the crystal configuration was established, a complete specification and statement of work for the crystals was prepared using the system optical error budget. Since the crystal is a transmission optic, it should normally be subject to the same tolerances as any other optic in the system. In consideration of the different manufacturing techniques needed for these crystals, as compared with conventional optical glass elements, the error budget allocated to the FCC's was relaxed somewhat. For example, surface roughness was budgeted at 50 Å (rms) because of the difficulty in finishing KDP due to its water solubility. (However, the vendor contracted to polish the Upgrade KDP has produced a sample of KDP polished to 10-Å roughness.) The statement of work for crystals calls out the following specifications for finishing:

Transmitted wavefront error	±1/10 wave
Flatness	±1/20 wave
Surface roughness	<50 Å (rms)

The vendors were required to submit plans for manufacturing, processing, cleaning, and testing each crystal prior to the start of manufacturing. Source inspection, or at a minimum, examination of vendor test data, ensures that each crystal is produced according to specification.

Since frequency conversion is key to the efficient drive of fusion targets, the remainder of the frequency-conversion subsystem required careful design to meet the system requirements. A dielectrically coated, linear polarizer with 500:1 contrast will be placed ahead of the FCC to produce the required polarization contrast at the FCC. LLE's Optical Manufacturing section has demonstrated the ability to produce polarizers of this type. All of the optical mounts, for both the



crystals and the polarizer, will have the same stability and flexibility as the most critical optical mounts in the system. The FCC control design provides for better than  $5\text{-}\mu\text{rad}$  tuning accuracy and provides for sensing of the crystal temperature, which facilitates control of the tuning angle as a function of temperature.

The FCC design includes an input window that serves two purposes: to absorb backscattered ultraviolet radiation (needed to protect the dielectric polarizer coating) and to act as a reflective alignment surface. Materials research at LLE helped determine the glass type to be used in this application; it is being manufactured to the same optical specifications as other optics.

#### 8. Periscope Mirror Assembly

The primary function of the periscope mirror assembly (PMA) is to inject a full-aperture UV laser beam into the UV portion of the beamlines to facilitate alignment of these beams onto the target. This is necessary because the fundamental laser wavelength (1054 nm), which is used to align the IR beamlines, is not efficiently transmitted by the UV transport optics.

The 300-mm UV alignment beam originates on the UVAT and may be injected into any of the 60 OMEGA Upgrade beamlines by two sets of mobile mirrors. Two identical systems for the north and south halves of the target bay are used to reduce alignment time and, more importantly, to create a continuous optical path through opposing beams. The latter facilitates performing a multitude of alignment and calibration procedures that require reflected and transmitted UV beams. Each of the two mirror sets comprises two mirrors that move independently to inject the UVAT beam into any of the 30 beamlines located on the north or south sides of the target bay. Figure 57.23 illustrates the principal features of the PMA that services the north segment of beamlines. (The south assembly is identical.)

PMA requirements were derived from the system-level, shot-cycle time and the pointing error budget. The following key requirements have received the closest attention and have been the main drivers in the evolution of the PMA design approach:

1. Average time to position the periscope mirrors and settle transients:  $\leq 15$  s
2. Alignment beam coarse positioning tolerance ( $3\sigma$ ): pointing  $\leq \pm 1.8$  mrad, centering  $\leq \pm 1.0$  mm
3. Alignment beam fine pointing ( $1\sigma$ ):  $\leq \pm 3\ \mu\text{rad}$

4. Alignment beam pointing stability: angular drift due to PMA effects must limit total excursion to within  $\pm 3.0\ \mu\text{rad}$  ( $1\sigma$ ) for a period of at least 40 s after acquiring the desired beam axis. Here, drift applies to

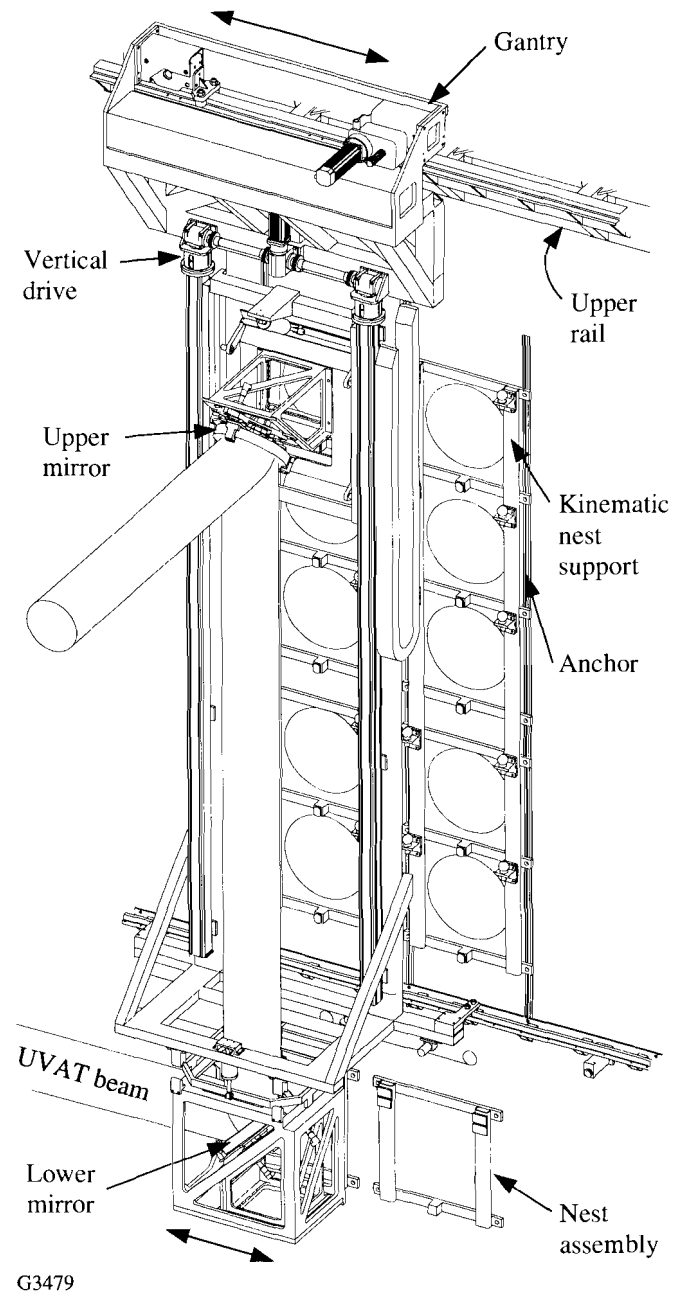


Figure 57.23

The major components for the north half of the periscope mirror assembly (PMA). The entire gantry (with the lower mirror attached) moves to each of the six columns of five beams. The upper mirror moves vertically to select a particular beamline.

beam displacements having frequency components less than 60 Hz.

Personnel safety was given highest priority followed by schedule, cost, and reliability. Also, target-bay space considerations mandated that the PMA be housed within a 1.2-m-wide corridor running along the west shield wall.

The pointing-stability requirement dictated most of this design. Based on a careful assessment of the expected shield-wall stability, kinematically ideal mounts were selected to support the periscope mirrors on the wall during alignment operations. This makes good use of the wall's great mass and intrinsic damping characteristics. Also, load paths from the periscope mirror through the mounts and into the wall were kept very short and stiff, thereby achieving high natural frequencies in spite of the large masses of the solid mirrors (5 cm × 35.5 cm × 51 cm). This avoids amplification of most wall-borne disturbances, thereby enhancing the mirror stability.

Two periscope mirror modules (PMM's), an upper and a lower, are carried by a gantry that is a major feature of each PMA system. The lower mirror directs the alignment beam to the upper mirror, which, in turn, reflects the alignment beam into the capture range of the F-ASP, i.e., into near coincidence with the desired beamline. Precision alignment with respect to the F-ASP is then accomplished by coordinated tip and tilt adjustments of both periscope mirrors using the F-ASP pointing and centering arms as references. The PMM's have built-in, two-axis micropositioners that operate under closed-loop servo control identical to those of the end and target mirrors.

A typical operational sequence for one of the gantries is as follows: Given a command from the host computer, the PMA local controller activates the horizontal drive and moves the gantry along the wall, stopping at the desired column of five beamlines. Centering and locking mechanisms are actuated to accurately position the gantry and lock it to the guide rails. While the gantry is traveling, the controller also activates a precision ball screw drive that moves the upper mirror vertically to the desired beamline. Both mirrors are then transferred to their respective kinematic nests on the shield wall and are released from mechanical contact with the gantry. This isolates the mirrors from disturbances that may otherwise be transmitted through the gantry structures. Using the F-ASP as a reference, the UV alignment beam is accurately coaligned with the primary beamline. Various alignment functions can then be performed on the UV transport system, many of which involve an ASP on the UVAT. When alignment opera-

tions at a particular beamline are complete, the mirrors are transferred back to their stowed positions aboard the gantry. The above sequence is repeated as needed for each of that gantry's 30 beamlines.

The time for repositioning at the next beamline is minimized ( $\leq 8$  s) by using an efficient path through each 30-beam array. Although the array measures about 3 m by 6.7 m, maximum transport velocity and acceleration are only 23 cm/s and 15 cm/s<sup>2</sup>, respectively. As a result, driving forces and transient disturbances are low despite the mass of the gantries (>900 kg each).

Coarse-positioning requirements will be met by surveying each kinematic nest into position using a surrogate mirror at each position in turn. The positional requirements in this case are well within the capabilities of current surveying practice.

For fine pointing, the PMM's incorporate the same design as the transport mirror mounts and TMM micro-positioners. To gain additional confidence, finite element analysis (TMM's) has been performed on those elements that differ somewhat from the TMM design. The deflection of the mirror surface figure is predicted to be less than 75 nm. A prototype is being constructed to verify mounting performance under PMA dynamic load conditions.

Many safety provisions have been factored into the PMA design: the PMA corridors will be fenced off with safety gates interlocked to PMA power; emergency stop lanyards will be installed inside the corridors; warning beacons and an audio alert will be activated during PMA transit; and mechanical sensors will be fitted on both sides of the gantries to provide emergency stops.

## 9. Focus Lens Assembly (FLAS)

The optomechanical requirements for the FLAS were determined by the optical design and the pointing error budget and are shown in Table 57.III.

The optical requirements for the FLAS were determined by the system requirements. The focus lens has a focal length of 1.8 m and functions at  $f/6$ . The lens and the separate vacuum window/blast shield produce less than a quarter-wave of aberration (at 351 nm) over a field of view (FOV) of  $\pm 2$  mm. The FLAS design provides a location, just ahead of the lens, for a phase-conversion plate, expected to be a plane-parallel, fused silica component ~300 mm in diameter and 25.4 mm thick. The optical design must also ensure that damage-causing ghost

Table 57.III Summary of Requirements for Focus Lens Assembly

Centration of lens to port axis	0.25 mm
Maximum <u>static</u> tilt of lens	0.28 mrad
Blast-window thickness	25 mm
Focus range	10 mm
Maximum transverse motion (over focus range)	1.6 $\mu\text{m}$
Additional focal shift	+10 cm
Transverse vibration	<0.6 $\mu\text{m}$
Axial vibration	2.5 $\mu\text{m}$
Focus accuracy	25 $\mu\text{m}$
Surface deformation	<100 nm
Vacuum differential (supported by blast window)	760 Torr
Note: Positive motion is <u>away</u> from the chamber center.	

reflections do not fall on any optics for any focus lens position (over a range of  $\pm 10$  mm).

The optical requirements were met with an aspheric singlet lens, designed to be free of spherical aberration when used in conjunction with a 25.4-mm-thick blast shield. The curvatures of the singlet were chosen to position the ghost reflections away from all optical components in the OMEGA Upgrade system. This selection of curvatures somewhat compromised the attainable FOV, as the lens shape that would maximize FOV (i.e., minimize coma) would have caused potentially damaging ghost reflections to fall on nearby optics. Despite this compromise, the FOV provided by the final design is  $\pm 4.5$  mm, significantly exceeding the original requirement.

The FLAS subsystem is shown in Fig. 57.24. The left side depicts the entire assembly including the blast-shield retraction mechanism. The right side depicts a cutaway of the focus-lens barrels and shows the position of the focus lens and blast shield.

The optomechanical design of the FLAS was driven primarily by the transverse motion tolerance of 1.6  $\mu\text{m}$  over the 10-cm focus range. Previous experience with OMEGA indicated that rolling bearings will not provide this accuracy. Designs incorporating flexures were found to possess insufficient stiffness to meet the requirements. The final design incorporates solid bearings consisting of polymer pads (i.e., Rulon™ or Vespel™) running against polished steel ways. Analysis shows that this design will provide sufficient stiffness and linearity of motion to satisfy the requirements.

To meet the centration requirements, as well as permit alignment of the focus axis to the center of the chamber, adjustments have been provided on the bearing pads. Datum surfaces on the end of the lens barrel will enable accurate location of the optical axis of the lens with respect to the axis of the focus motion on the mount, allowing alignment of both to the center of the chamber within tolerance.

One of the main challenges of this design was the additional requirement that the vacuum window, a 325-mm-diam  $\times$  25-mm-thick plano optic that also serves as the blast shield, be removed frequently for service. In operation, this optic will need to be changed or cleaned on a regular basis as it becomes contaminated and/or damaged. To achieve the necessary stiffness and pointing accuracy, the FLAS has to be fairly large; it nearly fills the space between the target chamber and the target mirror structure (TMS). As a result, space constraints in the vicinity of the target chamber make it impossible for one to reach in and remove the blast shield directly. A mechanism was designed that clamps and unclamps the blast-shield-to-target-chamber interface under remote control. This mechanism also transports the blast shield from the target chamber to the exterior of the TMS, where it can be grasped and removed. The mechanism works in reverse to return a blast shield from the outside face of the TMS to the target chamber, where it is correctly positioned and clamped to initiate the vacuum seal.

### Major Structures Design

The major structures produced for the Upgrade include laser bay structures (23 unique designs, 74 total structures) and target bay structures (8 unique designs, 19 total structures).

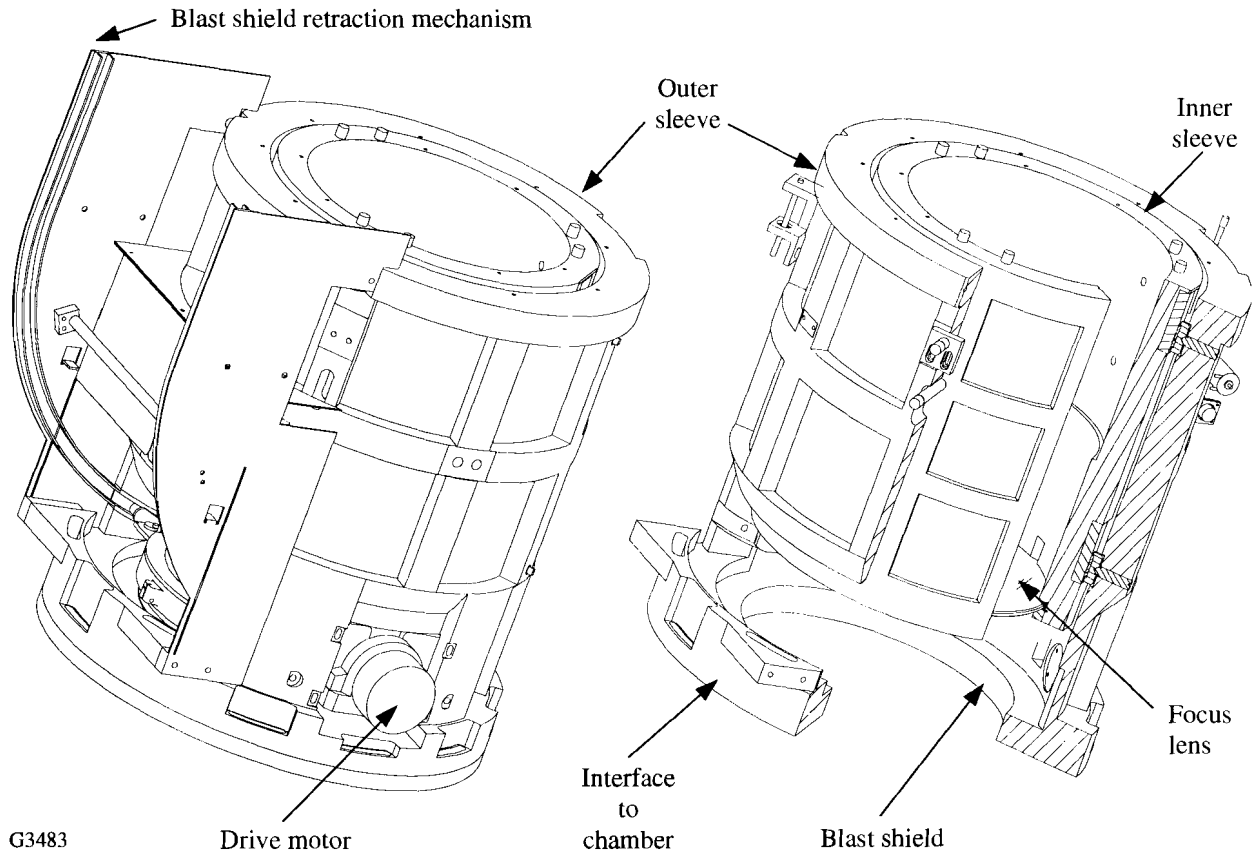


Figure 57.24

The focus lens assembly (FLAS) for the OMEGA Upgrade. On the left is the entire assembly including the blast-shield retraction mechanism. On the right is a section of the two sleeves showing the position of the focus lens and blast shield.

The key structural design requirements were

- accurately located mounting surfaces for the optical components, diagnostics, and instrumentation,
- microinch and microradian stability to the bay's thermal and vibration environments, and
- packaging and servicing of the optical components and diagnostics within the constraints of the 60-beam configuration.

The approach used to mount and accurately position the optical components is as follows: (1) The structures are typically designed to be manufactured with critical mounting surfaces located to  $\pm 3$  mm relative to surveyor pads provided on the structures. (2) The structures will be surveyed into place to accuracies of  $\pm 3$  mm. (3) Finally, the optical components have been typically designed to provide  $> \pm 3$ -mm mounting

adjustment and/or excess clear aperture. This adjustment range/excess clear aperture is adequate to compensate for the structure's fabrication and installation tolerances, thus assuring that the optical system can be set up and aligned.

The requirements for pointing stability are among the most challenging. For reflective optics, allowable rotations of structural mounting surfaces are  $\pm 1.5 \mu\text{rad}$ , and for refractive optics, structural deflections must be within  $\sim 0.25 \mu\text{m}$ . These goals must be met given the following environmental conditions:  $\pm 1^\circ\text{C}$  temperature variations and vibration accelerations of up to  $20 \mu\text{g}$ , with major peaks at 15, 20, and 30 Hz. The basic structural approach uses massive, steel space-frame structures grouted to the floor and extensive finite element analysis. An example of this space-frame approach is the target mirror structure, which uses a 3-D "soccer ball" concept to accommodate the Upgrade's 60 laser beams and provide the needed stiffness and mounting surfaces.

One notable exception to the space-frame approach is the F-ASP structure. This unique structure serves as the pointing reference for the entire laser system and, as such, has exceptional stability requirements. Its off-axis optical system has also contributed additional unique requirements to the mechanical design. The approach has been to “cast” a structure around the optical system using a structural epoxy composite, a material commonly used for machine tool bases. This material and process provide a combination of high thermal and vibration damping with the ability to accurately mold critical off-axis optical mounting surfaces into the structure.

Servicing the laser and target systems is complicated by the requirement to package the Upgrade’s 60-beam laser into the facility built for the original 24-beam OMEGA system. This has resulted in structures ranging in height from 3.6 m to 9 m bordered by long aisle ways 1.2 m or less wide. One of the most difficult challenges involved servicing the disk amplifiers,

which are 2 m long and weigh nearly 450 kg. Each amplifier has 32 high-voltage electrical cables, each about 13 mm thick, plus numerous cooling and nitrogen-purge lines attached. Since complete amplifiers must be replaced on a routine basis, safety, reliability, and ease of operation were essential requirements of the design. The resulting structure design is a combination of swinging doors and an overhead crane (both integral parts of the structure) for service and removal of the amplifiers (see Fig. 57.25).

A rather challenging design task was the three-level platform (see Fig. 57.26) for servicing the target mirror structure and target chamber. Key issues were to avoid obstructing the many crossing laser beam paths (see Fig. 57.29) and provide room for the diagnostics, crane-load landing areas, work areas, and storage areas. All these had to be accommodated while maintaining safe access and egress for personnel.

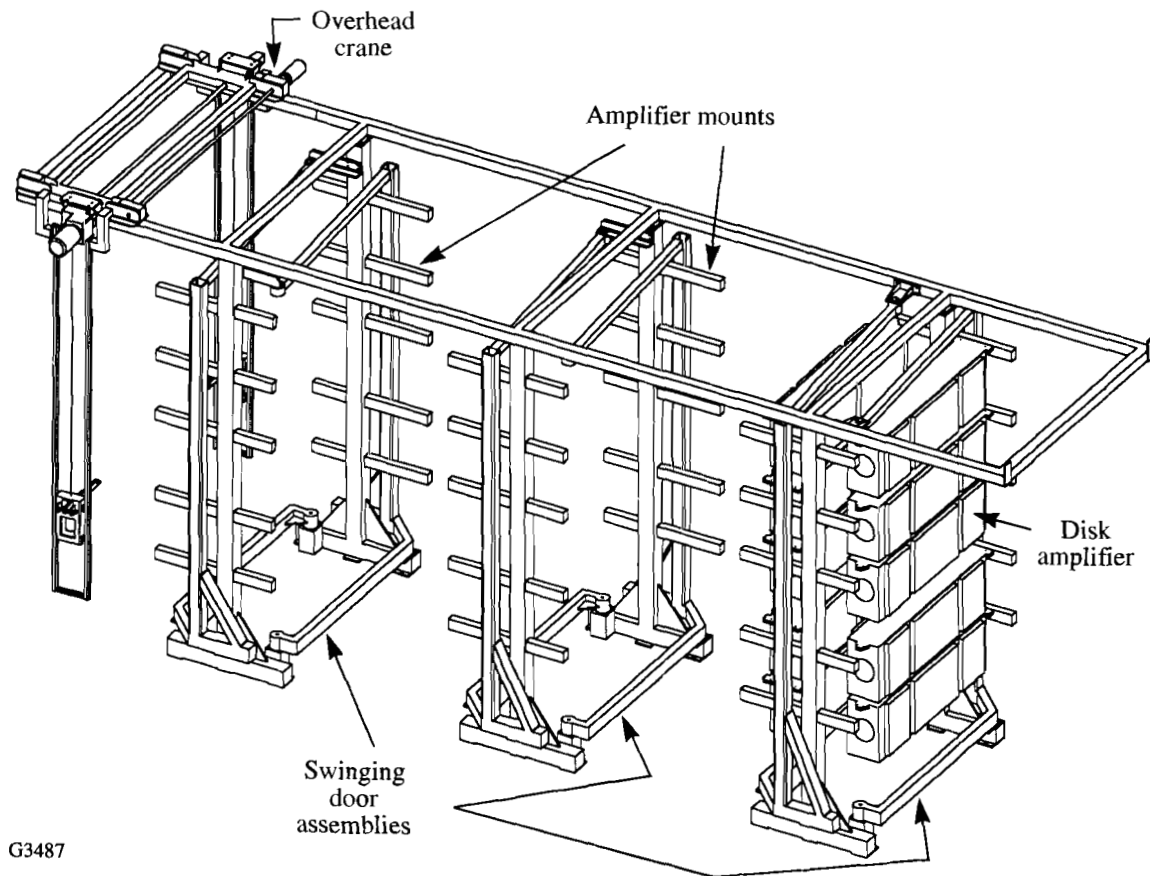


Figure 57.25 One of the four structures that support the stage-E and stage-F disk amplifiers. Each structure has six doors, each of which can swing out any or all of the five amplifiers, and a crane that lowers the amplifiers to floor level to facilitate routine maintenance.

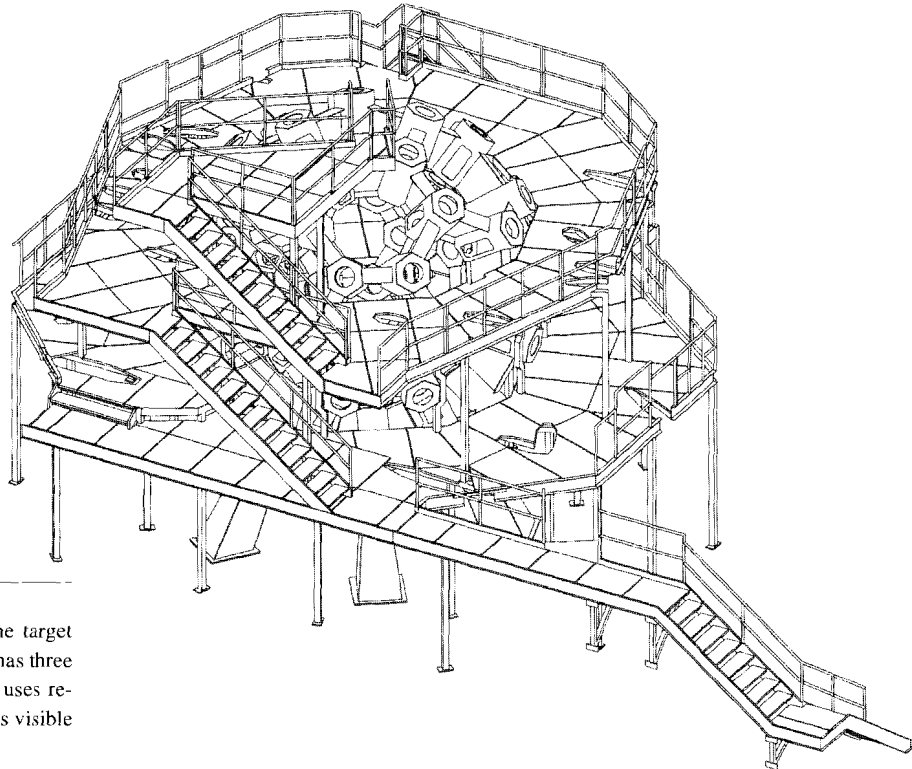


Figure 57.26

The personnel service platform for the target mirror structure (TMS). The platform has three levels, is isolated from the TMS, and uses removable grids for flooring. The TMS is visible within the platform structure.

### Target Area

The layout of the target area was dominated by the requirements to deliver 60 UV beams to the target chamber and to provide access to the chamber for implementation of experimental devices on the target chamber. It is in the target bay where the use of the existing building constrained the design the most.

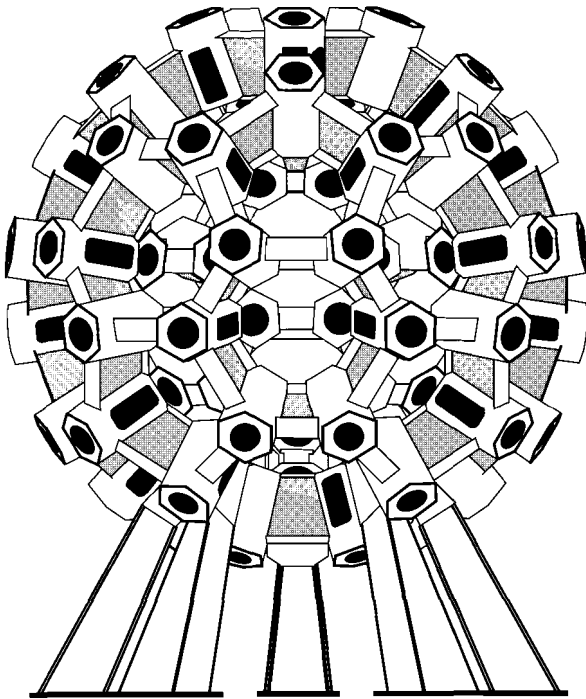
The target mirror structure (see Fig. 57.27) is highly modular, with five-fold rotational symmetry about the vertical axis reflecting the soccer-ball symmetry, i.e., 20 hexagons and 12 pentagons. The 60 laser beams are located at the vertices of those polygons. The laser beams are directed through hexagonal tubes that are part of the structure. The design provides for segmented personnel platforms and integrates the optical mounts with structurally rigid, hexagonal beam tubes. The target mirrors are mounted on the ends of these beam tubes. The structure has a 6-m diameter, with the target mirrors centered on a 7.2-m diameter. The beam-transport geometry is such that no angle of incidence, at either an end mirror or a target mirror, exceeds  $60^\circ$ . The end mirrors are held on two, separate, space-frame structures. Surrounding the TMS is a three-level personnel platform that provides access to the ports on the chamber, landing points for crane-hoisted mate-

rial, and mounting points for ancillary diagnostic support systems (see Fig. 57.26).

The Upgrade's target-area design actually allows a greater free volume for the placement of diagnostic instruments than was the case on OMEGA because in the Upgrade the beams are transported to the TMS from the outside rather than between the target mirrors and the target chamber.

The UV transport system utilizes two mirrors per beam to direct the beam to the target. The two-mirror configuration was chosen for economy and to reduce the in-air path length of the UV beam. The latter was needed to ensure that the intensity-length product for the beam was below the threshold for stimulated rotational Raman scattering (SRRS).<sup>7</sup> Since UV light is used to align the UV transport system, the optical coatings for the transport mirrors can be optimized for UV radiation only. In the previous system the mirrors had to reflect a nominal amount of IR energy. Relaxing this requirement has allowed the design of the mirrors to provide maximum damage resistance.

The task of mapping the 60 nearly parallel beamlines to the spherical target geometry had two fundamental constraints:



G3115

Figure 57.27

The target mirror structure (TMS) has the soccer-ball geometry defined by the beam positions. The target chamber is supported and enclosed by the TMS. Each of the 60 beams enters the TMS through the radial hexagonal tubes. The 32 diagnostic ports are located in the hexagons and pentagons of the TMS.

All 60 beams should have nearly equal path lengths, and no incident angle (on the mirrors) could be greater than  $60^\circ$ . Given these constraints it is a straightforward process to map a beam to a target port and then locate the end mirror along the beamline to obtain the proper path length.

For the sake of irradiation uniformity, an additional optimization was imposed upon the mapping. This entailed reducing the proximity of beams that share the same stage-A amplifiers. This is to reduce the effect any variation in the performance of a single, stage-A amplifier (distributed into 20 beams) has on target irradiation uniformity. A mapping that grouped many such beams in one area of the target would accentuate the effect a stage-A amplifier has on target performance. To mitigate this effect the beam mapping was arranged such that, for a given hexagon on the TMS, no more than three beams share the same stage-A amplifier. For the pentagons, only two such beams are allowed. Figure 57.28 is a sinusoidal projection of the beam

locations indicating which beams share each of the three stage-A amplifiers.

The beam paths, as mapped by the above constraints, are shown in Fig. 57.29. The convergence of 60 beams in the existing target bay leads to a high density of beams. The need to place structures and mirror mounts in that volume without obstructing any beam is a significant design constraint. Extensive 3-D CAD models were required for nearly every design task in this area.

### 1. Target Chamber

Located within the TMS is the 3.3-m-diam target chamber. The chamber was fabricated to high tolerance, which allows it to be used as an alignment reference for construction of the TMS and the installation and alignment of the target mirrors and FLAS. Post-fabrication measurements indicate that the target chamber ports are positioned to better than  $\pm 75 \mu\text{rad}$ , which is a factor of 2 better than the specification.

Note: The following systems are not part of the OMEGA Upgrade Project; rather, they will be completed as part of the LLE mission. A brief description of these systems is provided for completeness.

### 2. Target Chamber Vacuum System

During shot operations, the target chamber will be maintained at a vacuum  $< 6 \times 10^{-6}$  Torr. The vacuum system is fully redundant, with a pair of three-stage, 2000-CFM roughing pumps and three closed-cycle helium cryogenic pumps. When necessary, the chamber will be vented to atmosphere with dehumidified air. The vacuum system will be controlled by a programmable-logic-controller (PLC)-based, distributed control system interfaced to the experimental-system executive computer. The main vacuum system will be capable of pumping the target chamber from atmospheric pressure to shooting vacuum ( $< 9 \times 10^{-6}$ ) in under 60 min. The redundant design of this system will support experiments with extremely long durations at high vacuum.

### 3. Target Positioning/Viewing

Ambient-temperature targets of all foreseeable configurations will be positioned by a multiaxis, air-locked target positioner and a multiaxis, optical target-viewing system. Each of the two target-viewing systems features a variable-magnification telescope and an actively configurable reticle. Multiple image detectors on each channel will be supported.

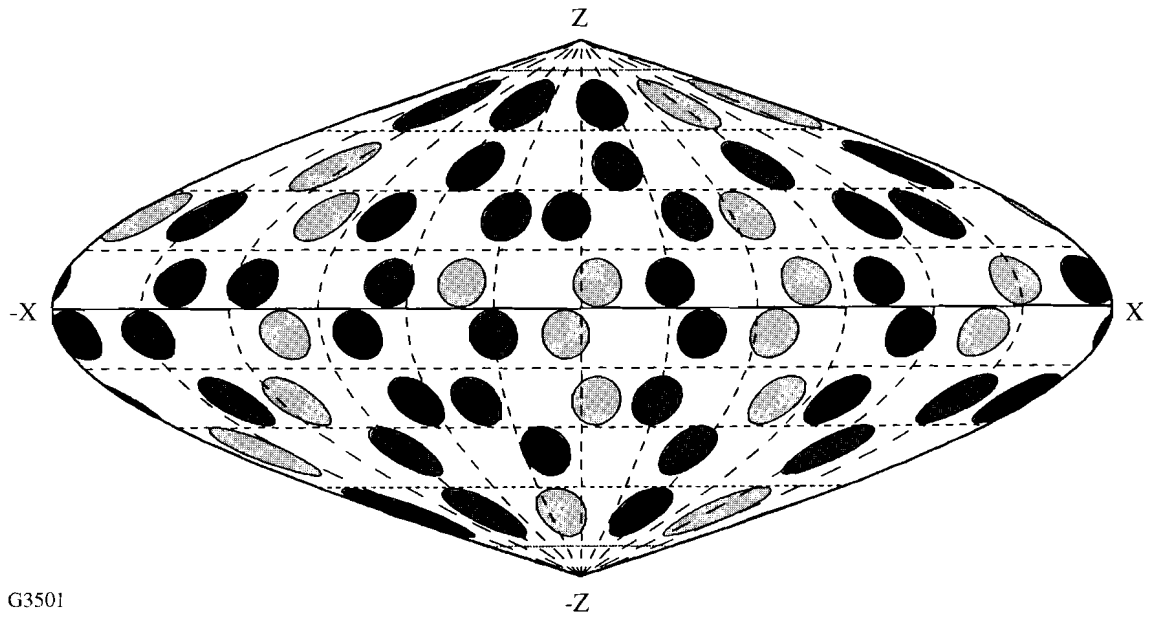
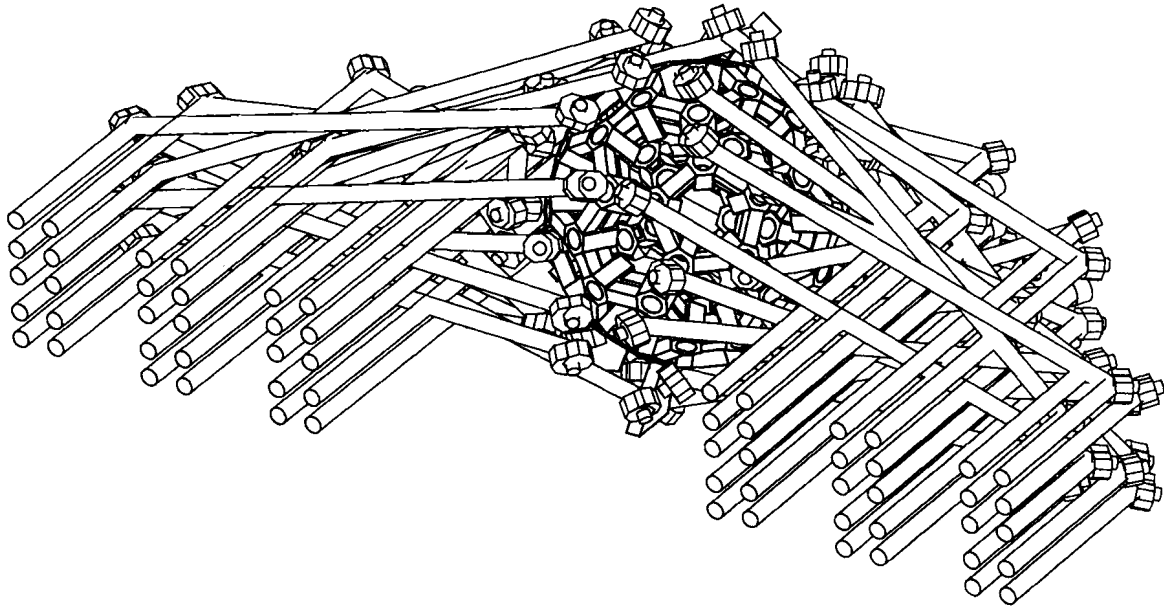


Figure 57.28  
 A sinusoidal projection of the beam locations on the OMEGA Upgrade target sphere. Each beam is identified by the stage-A amplifier (3 in total) from which it originates. The beam mapping was arranged so that any given TMS hexagon has at most three beams originating from the same stage-A amplifier; the pentagons have at most two beams.



G3160

Figure 57.29  
 The beam paths of the UV transport system of the OMEGA Upgrade. Each beamline has two mirrors, an end mirror and a target mirror. Care was taken to ensure that all path lengths were nearly equal and that the angle of incidence on all mirrors was  $< 60^\circ$ .



The target-viewing system will employ sophisticated image-processing techniques to provide enhanced-open-loop and automated-closed-loop target-positioner operation. The load/lock target positioner will allow selection of any target in the LLE inventory and thus will support long-duration, continuous experimental operations.

The integrated target-viewing and positioning system will allow placement of the target within a 5- $\mu$ m radius of the designated center of the target chamber under either manual or automatic control.

#### 4. Diagnostic Support Systems

Target diagnostic systems will be supported on the OMEGA Upgrade by an array of modular support systems, including mechanical interfaces, timing, vacuum, power, and control system support. The standardized interface scheme employed in the OMEGA Upgrade experimental support systems provides for simplified compatibility requirements for NLUF users and a readily reconfigurable experimental system to support future experimental programs. The diagnostics to be used on the Upgrade are not within the scope of this project. Information on these systems can be found in the LLE five-year plan.<sup>8</sup>

#### ACKNOWLEDGMENT

This work was supported by the U.S. Department of Energy Office of Inertial Confinement Fusion under Cooperative Agreement No. DE-FC03-92SF19460 and the University of Rochester. The support of DOE does not constitute an endorsement by DOE of the views expressed in this article.

#### REFERENCES

1. R. S. Craxton, ed., *OMEGA Upgrade Preliminary Design*, Laboratory for Laser Energetics Report DOE/DP 40200-101, University of Rochester (1989).
2. Optics Coating Requirements Document, OMEGA Upgrade No. M-AA-G-05, Rev A, 12 October 1992.
3. LLE Review **44**, 219 (1990).
4. LLE Review **51**, 139 (1992).
5. Optical Coating Specification Document, OMEGA Upgrade No. M-AA-G-07, 28 April 1993.
6. R. S. Craxton, *IEEE J. Quantum Electron.* **QE-17**, 1771 (1981).
7. M. A. Henesian, C. D. Swift, and J. R. Murray, *Opt. Lett.* **10**, 565 (1985).
8. Proposal for Renewal Award for Cooperative Agreement DE-FC03-85-DP402000 (US DOE/LLE, October 1991), Chaps. 3.3 and 3.4.